NANO LETTERS

2008
Vol. 8, No. 8
2541-2546

Programmable Hierarchical Three-Component 2D Assembly at a Liquid−Solid Interface: Recognition, Selection, and Transformation

Shengbin Lei,[†] Mathieu Surin,[‡] Kazukuni Tahara,[§] Jinne Adisoejoso,[†] Roberto Lazzaroni,*[,‡] Yoshito Tobe,*[,§] and Steven De Feyter*[,†]

Department of Chemistry, Division of Molecular and Nanomaterials, Laboratory of Photochemistry and Spectroscopy, and INPAC - Institute for Nanoscale Physics and Chemistry, Katholieke Universiteit Leuven (KULeuven), Celestijnenlaan 200 F, B-3001 Leuven, Belgium, Service de Chimie des Matériaux Nouveaux, Université de Mons-Hainaut, 20, Place du Parc, B-7000 Mons, Belgium, and Division of Frontier Materials Science, Graduate School of Engineering Science, Osaka University, Toyonaka, Osaka 560-8531, Japan

Received June 10, 2008; Revised Manuscript Received June 30, 2008

ABSTRACT

Recognition and selection are of fundamental importance for the hierarchical assembly of supramolecular systems. Coronene induces the formation of a hydrogen-bonded isophthalic acid supramolecular macrocycle, and this well-defined heterocluster forces, in its turn, DBA1 to form a van der Waals stabilized honeycomb lattice, leading to a three-component 2D crystal containing nine molecules in the unit cell. The recognition and selection events enable efficient error correction and healing in redundant mixtures.

Self-assembly of nanometer-sized building blocks at surfaces and interfaces is of increasing interest for nanotechnology research due to potential applications for nanopatterning, surface templating, heterogeneous catalysis, and sensing.[1–4] Gaining control of molecular ordering on surfaces is therefore an active field of research. Supramolecular chemistry is a powerful methodology to create such controlled assembly of nanostructures following bottom-up principles.[5] Typically, structural and functional information stored in the (molecular) building blocks is expressed in self-assembled structures via programmed (directional) noncovalent interactions. Nanostructures of high complexity at surfaces can be fabricated using appropriately designed building blocks, under ultrahigh vacuum conditions (UHV),[6] in ambient conditions[1] or at liquid−solid interfaces,[7b,8] by tuning the hierarchical intermolecular interactions.

The formation of crystalline multicomponent two-dimensional (2D) lattices, containing more than two different organic molecular building blocks, has been achieved rarely[9] since optimized recognition and selection processes[10,11] are required to achieve the targeted multicomponent surface-confined patterns. The melamine−PTCDI hydrogen-bonded porous network of which the pores are filled by C_{60} heptamers is a particularly nice example. However, such a well-defined multicomponent structure was not reported to form upon simultaneously bringing all components to the surface.[9]

Chart 1. Chemical Structures of **DBA1, DBA2**, Isophthalic Acid (**ISA**), Trimesic Acid (**TMA**), and Coronene (**COR**)

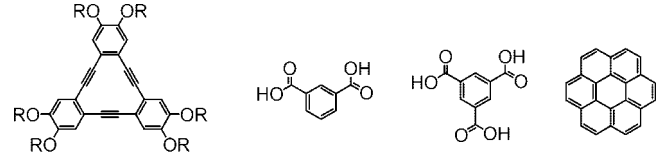

DBA1, R= $C_{10}H_{21}$
DBA2, R= $C_{12}H_{25}$ ISA TMA COR

Herein, we report the modular hierarchical self-assembly of a three-component 2D crystal at the liquid−solid interface following a host−guest strategy, and we highlight the recognition and selection processes involved. (1) Coronene (Chart 1: **COR**) acts as a molecular template directing the assembly of isophthalic acid (Chart 1: **ISA**) as the second component into a heteromolecular cluster, $\mathbf{COR_1}$−$\mathbf{ISA_6}$,

* To whom correspondence should be addressed. E-mail: roberto@averell.umh.ac.be (R.L.); tobe@chem.es.osaka-u.ac.jp (Y.T.); Steven.DeFeyter@chem.kuleuven.be (S.D.F.).
[†] Katholieke Universiteit Leuven.
[‡] Université de Mons-Hainaut.
[§] Osaka University.

10.1021/nl8016626 CCC: $40.75
Published on Web 07/16/2008

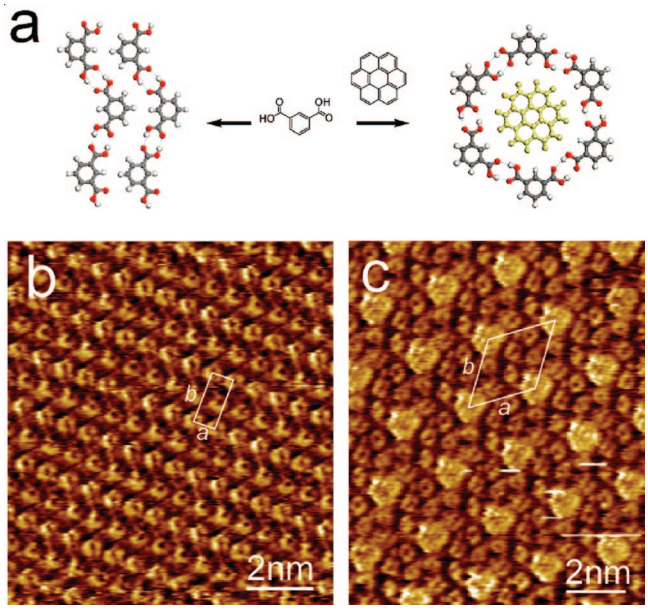

Figure 1. (a) Molecular mechanics (MM)-optimized structures of (left) the "zigzag" pattern of **ISA** and (right) the **COR**-templated assembly of **ISA** (**COR**$_1$−**ISA**$_6$). (b,c) STM images recorded at the 1-octanoic acid/graphite interface of self-assembled patterns of **ISA** (b) in the absence of **COR** (I_{set} = 387 pA, V_{set} = −0.75 V) and (c) in the presence of **COR** (I_{set} = 530 pA, V_{set} = −1.00 V). Solutions are saturated.

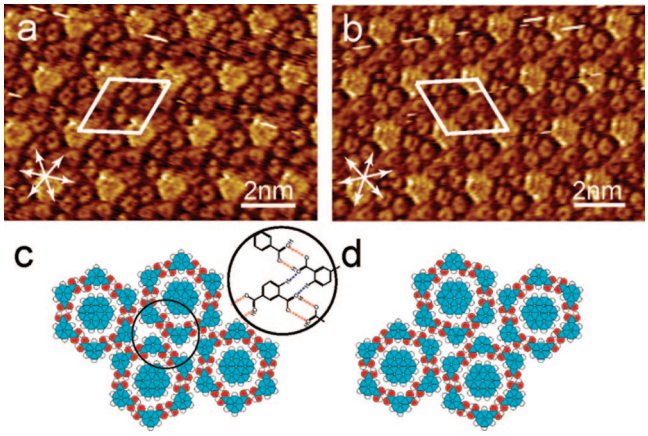

Figure 2. (a,b) STM images at the 1-octanoic acid/graphite interface (I_{set} = 453 pA, V_{set} = −1.00 V for image a and I_{set} = 305 pA, V_{set} = −1.02 V for image b) of domains of different supramolecular chirality formed by a templated assembly of **ISA** with **COR** and (c,d) the corresponding molecular models. The equivalent ⟨1 1 −2 0⟩ directions of the graphite lattice are indicated in the lower left corner of the STM images. Unit cells are indicated in white. Possible weak intercluster C−H···O hydrogen bonds (blue dotted lines) are indicated in the black circle.

(Figure 1), of defined size, symmetry and composition. (2) An alkoxylated dehydrobenzo[12]annulene (Chart 1: **DBA1**) hosts this **COR**$_1$−**ISA**$_6$ heteromolecular cluster to form a well-ordered three-component 2D crystal (Figure 3), containing nine molecules in the unit cell. Actually, the heteromolecular **COR**$_1$−**ISA**$_6$ cluster templates the assembly of **DBA1** into a honeycomb network as **DBA1** by itself forms a different denser pattern under the experimental conditions. Regardless of the fact if the components are premixed in solution or are consecutively added to the surface, the three-component 2D crystal is formed. Dynamic equilibrium conditions are met. (3) Interestingly, the honeycomb **DBA1** matrix is "selective"; it hosts exclusively heteromolecular clusters of the composition **COR**$_1$−**ISA**$_6$, even in the presence of other related molecular building blocks such as trimesic acid (Chart 1: **TMA**). (4) Moreover, **DBA2** (Chart 1), which forms a slightly larger cavity because of the longer alkoxy side groups, is not able to host or immobilize **COR**$_1$−**ISA**$_6$ clusters. (5) Finally, the addition of **DBA1** to a preformed pattern formed from a mixture of **TMA**, **ISA**, and **COR** is able to "extract" **ISA** from the **TMA**−**ISA**−**COR** monolayers, and as such, **DBA1** plays a cleaning role by selectively removing and hosting **ISA** in the presence of **COR**, demonstrating the peculiar stability of the **DBA1**−**ISA**−**COR** motif.

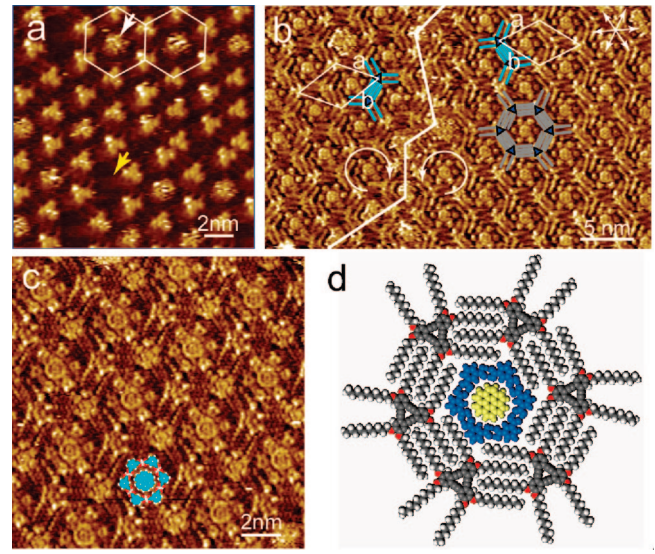

Figure 3. (a,b) STM images of **DBA1** at the 1-octanoic acid/graphite interface (a) in the absence and (b) in the presence of **ISA** and **COR**. (a) The yellow arrow points to a distorted honeycomb cavity, while the white arrow highlights a **DBA** molecule self-trapped in a honeycomb cavity (I_{set} = 28 pA, V_{set} = −1.10 V). (b) After addition of **ISA** and **COR**, a complex supramolecular tricomponent architecture forms (I_{set} = 258 pA, V_{set} = −1.04 V). Domains of different chirality arise as a result of the interdigitation of the alkyl chains of the **DBA1** host. The border between two chiral domains is indicated. The orientation of the unit cell vectors is determined to be 21 ± 3°, either clockwise or counterclockwise with respect to the main lattice axis ⟨1 1 −2 0⟩ of graphite. The orientation of the graphite lattice is shown in the upper right corner of (b). (c) The high-resolution image of the tricomponent architecture shows submolecular detail of the **COR**$_1$−**ISA**$_6$ cluster (I_{set} = 17 pA, V_{set} = 1.04 V). A model of the **COR**$_1$−**ISA**$_6$ cluster is overlaid on the image to guide the eye. (d) Molecular model of the three-component hierarchical assembly, as optimized on graphite with MM. Concentration: **DBA1**, 8 × 10^{-5} mol/L; **ISA** and **COR** are saturated.

Monocomponent Supramolecular Assembly: Isophthalic Acid. Considering the typical hydrogen bonding (H-bond) interactions between carboxylic acid (−COOH) groups, **ISA** is predicted to assemble into a zigzag chain ("trans") or into a cyclic hexamer ("cis"), as shown in Figure 1a. When allowed to assemble at the 1-octanoic acid/graphite interface, **ISA** forms zigzag chains which further assemble into 2D crystalline domains via van der Waals interactions. **ISA**

molecules are resolved as small bright circles with a diameter of about 0.7 nm in the scanning tunnelling microscopy (STM) images (Figure 1b). A close-packed monolayer is formed, and the unit cell parameters are $a = 0.69 \pm 0.05$ nm, $b = 1.52 \pm 0.07$ nm, and $\alpha = 90 \pm 4°$ (plane group: $p2$).[12]

Bicomponent Supramolecular Assembly: Isophthtalic Acid−Coronene. When **COR** is present in solution, a dramatic difference is observed (Figure 1c). The self-assembly pattern belongs now to plane group $p6$, and the unit cell parameters are determined to be $a = b = 2.31 \pm 0.04$ nm and $\alpha = 60 \pm 1°$. The repetitive unit contains one big bright disk (~1 nm in diameter) surrounded by six small, less bright circles. This is interpreted as a **COR** molecule which is surrounded by a cyclic hexamer of **ISA** molecules. The six **ISA**s are held together by, in total, 12 hydrogen bonds. The interactions between the **ISA** rosette and **COR** are mainly van der Waals (Figure 1a).[13] These heteroclusters further assemble into 2D close-packed domains through van der Waals interactions.

It does not come as a surprise that **ISA** itself does not form cyclic hexamers at the liquid−solid interface. Molecular modeling simulations show that the total stabilization by H-bonding is almost identical for the experimentally observed zigzag motif and the nonobserved cyclic hexamer network since, in both cases, **ISA** forms four hydrogen bonds with its neighbors (Supporting Information). Neglecting any potential stabilizing effects by solvent molecules or by **ISA** molecule(s) adsorbed in the cavity of such a cyclic hexamer network, the latter is clearly less stable than the zigzag pattern because its adsorption energy per unit area is smaller.

Molecular mechanics (MM) calculations (with the PCFF force field, see SI) support the formation of heteromolecular clusters upon mixing of **COR** and **ISA**. MM indicates that there is a significant stabilizing interaction between **COR** and the surrounding **ISA** molecules (−13 kcal/mol; see also the table in the Supporting Information), reflecting the perfect accommodation (structural fit) of **COR** into the cavity of the cyclic **ISA** hexamer, sterically constraining it. Moreover, MM shows that **COR** can adopt an epitaxial orientation on graphite due to π-stacking. Therefore, **COR** is a proper molecular "template" to induce the transformation of the monocomponent **ISA** zigzag network into a 2D crystalline bicomponent network of heteromolecular $\mathbf{COR_1}-\mathbf{ISA_6}$ clusters. A related "template"-induced transformation was recently reported.[14]

The shape of **COR** is well-resolved in the STM images, showing even submolecular details, indicating that **COR** molecules are immobilized and not rotating within the pore,[15] in line with the MM calculations (Supporting Information). The immobilization of **COR** in the cyclic **ISA** hexamer is further confirmed by molecular dynamics (MD) simulations. When keeping the position of the **ISA** molecules fixed according to the optimized H-bonding network, **COR** shows very small lateral displacements, with its molecular plane remaining parallel to the graphite sheets. The standard deviation of the displacement of **COR** during the MD simulation is only ±0.2 Å. Interestingly, there is no rotation of **COR** inside of the cavity during the MD simulation, although the MD time scale (300 ps) is large compared to a typical rotation time (a few ps) (Supporting Information). **COR** is stabilized into the **ISA** matrix by the geometrical match within the **ISA** cyclic hexamer and by its strong π-stacking interaction with the graphite substrate.

Finally, we remark that the 2D patterns are chiral (Figure 2). Different from previous reports on chiral assemblies composed of achiral molecules, here, chirality is only expressed at the highest level of the hierarchical self-assembly process, that is, the 2D pattern formation of the achiral bicomponent supramolecular clusters.[16,17] Different from the chiral patterns formed by (pro)chiral building blocks,[16,17] neither **ISA** nor **COR** nor the heteroclusters themselves are (pro)chiral. It is the relative shift of the heteroclusters in the 2D lattices, maximizing the molecular density and intermolecular interactions, that leads to chiral domains. By imaging the graphite lattice underneath, the relative orientation of the patterns with respect to the substrate have been determined. This analysis reveals that the unit cell vectors of these domains are rotated by $10 \pm 2°$, either clockwise (+10°) or counterclockwise (−10°), with respect to the main lattice axis $\langle 1\ 1\ -2\ 0 \rangle$ of graphite. Therefore, chirality is expressed at two levels, the monolayer symmetry and monolayer substrate orientation.

Three-Component Supramolecular Assembly: Isophthalic Acid−Coronene−DBA. Alkoxylated dehydrobenzo[12]annulenes (**DBA**s) are reported to assemble into either close-packed linear/hexagonal or nanoporous honeycomb patterns, depending on the solvent and concentration.[18,19] At the 1-octanoic acid/graphite interface, **DBA1** forms a close-packed pattern with some distorted honeycomb defects (marked with the yellow arrow in Figure 3a) in the concentration range from 8×10^{-4} to 8×10^{-6} mol/L. Most of the **DBA** cores appear with a clear triangular shape, but some of them appear fuzzy (the white arrow in Figure 3a). We attribute these fuzzy ones to mobile **DBA** molecules self-trapped in the honeycomb cavities.

When a drop of octanoic acid solution containing **ISA** and **COR** is added to the preassembled **DBA** pattern, a structural transformation is observed; the **DBA** network transforms from a close-packed network to a 2D honeycomb pattern, and $\mathbf{COR_1}-\mathbf{ISA_6}$ clusters fill the honeycomb cavities (Figures 3b and c). All of the clusters have identical composition and symmetry. The experimental data, supported by MM calculations, show that the **ISA** molecules, in their hexagonal H-bonded arrangement, are locked in position at the end of **DBA1** alkyl groups. The unit cell parameters are $a = b = 4.1 \pm 0.1$ nm and $\alpha = 60 \pm 1°$ (Figure 3b) (plane group $p6$). On one hand, the total H-bonding interactions (as estimated with the Dreiding force field) are identical to that of the pure **ISA** cyclic hexamer, that is, around −44 kcal/mol (for 12 H-bonds). This highlights the perfect structural accommodation of the H-bonded hexamer made of **ISA** (and its **COR** guest) into the **DBA1** network. On the other hand, adsorption of the $\mathbf{COR_1}-\mathbf{ISA_6}$ clusters in the voids does not affect the intrinsic honeycomb-forming characteristics of **DBA1**. The unit cell parameters are identical to those of self-

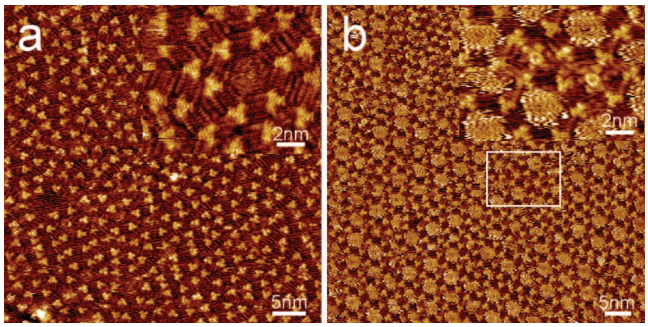

Figure 4. (a) Assembly of **DBA2** at the 1-octanoic acid/graphite interface (I_{set} = 328 pA, V_{set} = −0.74 V). The inset is a high-resolution image of a honeycomb. (b) Host−guest architecture formed by coadsorption of **DBA2** with **ISA** and **COR** (I_{set} = 920 pA, V_{set} = −0.87 V). The cavities appearing fuzzy are believed to be occupied by mobile **COR**. The inset is a high-resolution image corresponding to the area marked by the white rectangle. Concentration: **DBA2**, 7 × 10^{-5} mol/L; **ISA** and **COR** are saturated.

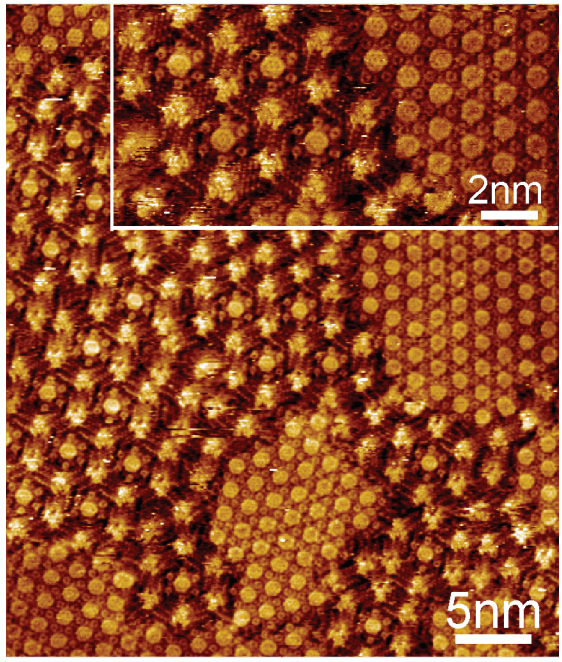

Figure 5. High-resolution STM image obtained after adding **DBA1** (8 × 10^{-5} mol/L) to an already equilibrated surface pattern formed by a **TMA/ISA/COR** mixture (**TMA**, **ISA**, and **COR** are saturated) at the 1-octanoic acid/graphite interface (I_{set} = 189 pA, V_{set} = −1.00 V). High-quality **TMA**−**COR** domains (inset right), free of any **ISA** molecules, coexist with porous **DBA1** domains filled with **COR_1**−**ISA_6** clusters.

assembled patterns of **DBA1** at the 1,2,4-trichlorobenzene/graphite interface where **DBA1** is known to self-assemble exclusively into a honeycomb type pattern, even in the absence of guests.[18] **COR_1**−**ISA_6** clusters fit perfectly in the hexagonal cavity formed by **DBA1** molecules, leading to an appreciable interaction between the **DBA1** host and the **COR_1**−**ISA_6** supramolecular guest, around −18 kcal/mol. The submolecular resolution of **COR** and the **ISA** molecules in the host−guest matrixes confirms that they are immobilized and that no rotation happens. Note that the **ISA** hexamer involves hydrogen bonding, while the surrounding **DBA1** network is stabilized by van der Waals interactions; different noncovalent interactions are at play at the two hierarchical assembly levels.

This three-component system is chiral too. Figure 3b displays a domain boundary with mirror image domains. Due to the offset between the alkyl chains of interdigitating molecules (see, for instance, the inset in Figure 3b and models in Figure 3d), the pore is obviously chiral, a characteristic which is extended at the level of the 2D network and at the level of the registry of the 2D network with respect to the lattice of the graphite substrate underneath. This analysis reveals that the unit cell vectors of these domains are rotated by 21 ± 3°, either clockwise (+21°) or counterclockwise (−21°), with respect to the main lattice axis ⟨1 1 −2 0⟩ of graphite. Therefore, chirality is expressed in two different ways, the monolayer symmetry and monolayer substrate orientation.

Guest-Induced Structural Transformations. The structural transformation from a nonporous to porous network in response to the presence of guest molecules has been observed before for alkoxylated **DBA**s[20] and other alkylated and nonalkylated compounds.[8g,14] Some of these alkoxylated and alkylated systems show concentration-dependent polymorphism. At "high" concentrations, a dense nonporous pattern is formed at the liquid−solid interface, while at low concentrations, porous matrixes are formed.[19] However, patterns that are intrinsically nonporous at a given concentration can be transformed into the porous network upon adding an appropriate guest. Such transformations are explained by the gain in energy resulting from guest−substrate interactions, increased host−substrate interactions in case of **DBA**s (six alkyl chains adsorbed instead of four), and host−guest interactions which overcome the loss of stability inherent to the formation of "voids" and low-density host matrixes.[20] In addition, the host−guest networks must be more stable than the formation of phase-separated nonporous host and pure guest phases. Addition of **ISA** alone does not induce the structural transformation of the **DBA1** host matrix (Supporting Information). Addition of an excess of **COR** (in the absence of **ISA**) leads to a complete structural transformation of the **DBA1** host matrix, but the **COR** molecules are mobile, and their orientation in the voids is not fixed. The situation obtained here is the first example of a structural transformation induced by a supramolecular guest entity, that is, a heteromolecular cluster, and is again evidence for the synergetic action of **ISA** and **COR** and the strong interaction between those two components.

Recognition and Selection. It is important to note that the sequence followed to add the three components to the surface does not affect the outcome of the self-assembly process (Supporting Information). Identical results are obtained upon premixing of the three components too, and the patterns are almost always observed within a few minutes after preparation of the sample, without showing any significant structural evolution as a function of time. This is a strong indication that the multicomponent architectures involving **DBA1**, **ISA**, and **COR** represent equilibrium structures. Furthermore, it suggests that recognition is involved between the heteromolecular cluster and the host

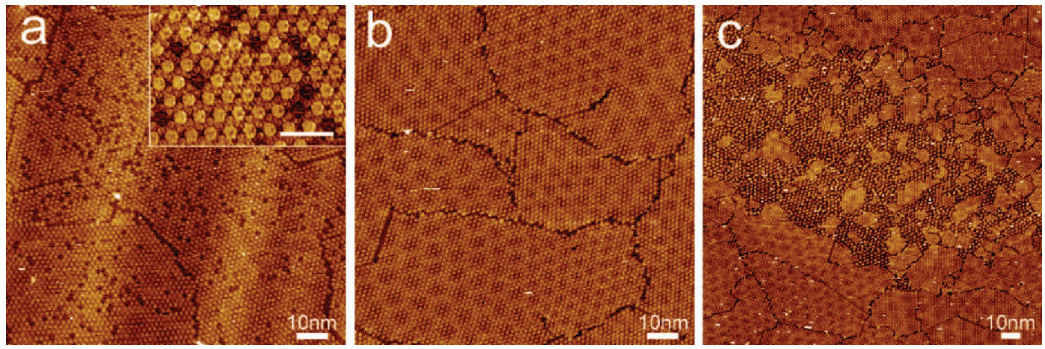

Figure 6. Large-scale image showing the assembling structure of the ternary mixture of **TMA**, **ISA**, and **COR** before (a) (I_{set} = 328 pA, V_{set} = −1.04 V) and after (b) addition of **DBA1** (I_{set} = 189 pA, V_{set} = −1.00 V). Before addition of **DBA1**, cavities filled with **ISA** can still be observed as defects (dark spots) (see the high-resolution image in the inset; the scale bar corresponds to 5 nm). However, after addition of **DBA1**, all of these defects disappear. A large-scale image where **DBA1** networks filled with $\mathbf{COR_1}-\mathbf{ISA_6}$ clusters are observed between domain boundaries of **TMA** networks is shown in (c) (I_{set} = 189 pA, V_{set} = −1.00 V).

matrix, possibly due to a selection process based on size and shape/symmetry commensurability of the cluster and cavity. To test this hypothesis, two control experiments were conducted.

First, the host properties of **DBA1** have been compared with those of **DBA2**, the analogue with longer alkyl chains, which intrinsically should give rise to larger cavities upon self-assembly. The **DBA2** host matrix is also transformed into a porous network upon adding an excess of **ISA/COR**. However, this transformation is most probably the result of the addition of **COR** itself and not the outcome of a heteromolecular complex activity involving **COR** and **ISA**. No well-ordered three-component assembly is observed. Only very few heteromolecular clusters are accommodated in some highly distorted cavities. The majority of the cavities appear fuzzy and featureless (Figure 4) and are possibly filled with **COR**, mobile **COR**−**ISA** clusters, or, with a low probability, only **ISA** clusters.[21,22] Only **DBA1** supports the uptake and stabilization of well-defined $\mathbf{COR_1}-\mathbf{ISA_6}$ clusters in its cavities.

Second, the competitive uptake of different cluster compositions by **DBA1** has been probed. Instead of **ISA/COR**, mixtures of **TMA/ISA/COR** were added. In the absence of **DBA1**, **TMA** is known to form well-defined heterocomplexes with **COR**, where **COR** is adsorbed within the voids of the H-bonded honeycomb network formed by **TMA**.[15] These voids are identical in size and composition to the **ISA** cyclic hexamer. However, if such a saturated **TMA/ISA/COR** mixture is added to a preformed **DBA1** nonporous matrix, the only surface pattern observed is identical to the previously described tricomponent 2D crystalline assembly of **DBA1** hosting $\mathbf{COR_1}-\mathbf{ISA_6}$ clusters. This means that **DBA1** is very selective with respect to the composition of the clusters it hosts. Only $\mathbf{COR_1}-\mathbf{ISA_6}$ clusters are selected, out of the numerous other possibilities with varying **ISA** and **TMA** compositions. This is confirmed by experiments where only **TMA/COR** is added to a **DBA1** monolayer. In addition to **TMA/COR** domains, porous **DBA1** domains are formed, but the content of the voids appears fuzzy, and no well-defined **TMA/COR** clusters are adsorbed. Most likely, the cavities contain only mobile **COR**. Such specific recognition at the level of the supramolecular host and efficient error correction compare beautifully with the selectivity expressed by enzymes.[23,24]

Dynamics and Healing. Saturated mixtures of **TMA** and **ISA** give rise to **TMA** honeycomb networks with, most probably, **ISA** molecules as guests in the cavities.[25] No pure **ISA** domains are observed, suggesting that the porous **TMA** network is more stable or its formation is kinetically favored compared to the **ISA** zigzag network. A saturated **TMA/ISA/COR** mixture initially leads to **TMA** host networks filled with **ISA** (kinetically favored) and occasionally **COR**. In time, **COR** replaces the trapped **ISA** molecules. Only at domain boundaries and if the cavity is occupied by **COR** can **TMA** host molecules be replaced by **ISA** host molecules (Supporting Information). Even after reaching equilibrium, cavities filled with **ISA** and **COR** still coexist. The surface composition and structures are therefore complex.

When **DBA1** is added after the ternary **TMA/ISA/COR** mixture has reached equilibrium, porous **DBA1** networks, filled with $\mathbf{COR_1}-\mathbf{ISA_6}$ clusters, are observed to occupy only a small fraction of the surface area, either at domain boundaries or by replacing small **TMA/COR** domains (Figure 5). However, a notable and clear change in the **TMA/COR** architecture is revealed upon addition of **DBA1**; all of the "defects", that is, **TMA** cavities filled with **ISA**, disappear, and the **TMA/COR** host−guest architecture becomes perfectly defect free. All guest sites are occupied by **COR** (Figure 6). This indicates that the presence of **DBA1** tends to release **ISA** guest molecules from the **TMA** network; in other words, it "cleans" **TMA** domains from **ISA** guest molecules. The fact that the **DBA1** domains filled with $\mathbf{COR_1}-\mathbf{ISA_6}$ clusters remain relatively small indicates that the **TMA** network is difficult to break apart once the H-bonded network is formed; it is kinetically stabilized. Needless to say, these experiments prove the dynamic nature of adsorption at the liquid−solid interface, a requisite for the formation of highly ordered surface patterns from complex solution mixtures.

In summary, we have demonstrated a successful multicomponent and hierarchical templating approach to construct a three-component crystalline lattice, involving both hydrogen bonding and van der Waals interactions. The efficient recognition and selection processes allow for a programmable

fabrication of highly complex hierarchical architectures. This approach paves the way for using the nanoporous **DBA** networks, for instance, as nanoreactors to create oligomers with well-defined size, symmetry, and composition.[3,26–28] Though maybe not very practical, **DBA** networks could also act as molecular sieves, that is, to "purify" a solution by retaining **ISA** molecules in the presence of **COR**. As demonstrated, thanks to the dynamic nature of the liquid−solid interface, often equilibrium conditions are met, facilitating the design and formation of complex highly ordered substrate-based patterns.

Acknowledgment. This work is supported by KULeuven, the Fund of Scientific Research − Flanders (FWO), the Belgian Federal Science Policy Office through IAP-6/27, the Belgian National fund for Scientific Research (F.R.S.-FNRS), the European Union Marie Curie Research Training Network CHEXTAN (MRTN-CT-2004-512161), and a Grant-in-Aid for Scientific Research from the Ministry of Education, Culture, Sports, Science and Technology, Japan. M.S. is Chargé de Recherches of the F.R.S.-FNRS. J.A. thanks the Institute for the Promotion of Innovation by Science and Technology in Flanders (IWT).

Supporting Information Available: Experimental details. This material is available free of charge via the Internet at http://pubs.acs.org.

References

(1) Barth, J. V.; Costantini, G.; Kern, K. *Nature* **2005**, *437*, 671.
(2) Hietschold, M.; Lackinger, M.; Griessl, S.; Heckl, W. M.; Gopakumar, T. G.; Flynn, G. W. *Microelectron. Eng.* **2005**, *82*, 207.
(3) (a) Piot, L.; Bonifazi, D.; Samori, P. *Adv. Funct. Mater.* **2007**, *17*, 3689. (b) Hulsken, B.; Van Hameren, R.; Gerritsen, J. W.; Khoury, T.; Thordarson, P.; Crossley, M. J.; Rowan, A. E.; Nolte, R. J. M.; Elemans, J. A. A. W.; Speller, S. *Nat. Nanotechnol.* **2007**, *2*, 285.
(4) (a) De Feyter, S.; De Schryver, F. *Top. Curr. Chem.* **2005**, *258*, 205, and references therein. (b) Chaki, N. K.; Vijayamohanan, K. *Biosens. Bioelectron.* **2002**, *17*, 1.
(5) Lehn, J. M. *Supramolecular Chemistry: Concepts and Perspectives*, Wiley-VCH: Weinheim, Germany, 1998.
(6) (a) Rosei, F.; Schunack, M.; Naitoh, Y.; Jiang, P.; Gourdon, A.; Laegsgaard, E.; Stensgaard, I.; Joachim, C.; Besenbacher, F. *Prog. Surf. Sci.* **2003**, *71*, 95. (b) Barth, J. V. *Annu. Rev. Phys. Chem.* **2007**, *58*, 375. (c) Hipps, K. W.; Scudiero, L.; Barlow, D. E.; Cooke, M. P. *J. Am. Chem. Soc.* **2002**, *124*, 2126. (d) Pawin, G.; Wong, K. L.; Kwon, K. Y.; Bartels, L. *Science* **2006**, *313*, 961. (e) Stepanow, S.; Lin, N.; Payer, D.; Schlickum, U.; Klappenberger, F.; Zoppellaro, G.; Ruben, M.; Brune, H.; Barth, J. V.; Kern, K. *Angew. Chem., Int. Ed.* **2007**, *46*, 710. (f) Bonifazi, D.; Kiebele, A.; Stöhr, M.; Cheng, F.; Jung, T.; Diederich, F.; Spillmann, H. *Adv. Funct. Mater.* **2007**, *17*, 1051. (g) Barrena, E.; de Oteyza, D. G.; Dosch, H.; Wakayama, Y. *ChemPhysChem* **2007**, *8*, 1915. (h) Zhang, H. L.; Chen, W.; Chen, L.; Huang, H.; Wang, X. S.; Yuhara, J.; Wee, A. T. S. *Small* **2007**, *3*, 2015.
(7) (a) Lei, S. B.; Wang, C.; Yin, S. X.; Bai, C. L. *J. Phys. Chem. B* **2001**, *105*, 12272. (b) Lei, S. B.; Yin, S. X.; Wang, C.; Wan, L. J.; Bai, C. L. *Chem. Mater.* **2002**, *14*, 2837. (c) Yang, Y.; Wang, C. *Int. J. Nanotechnol.* **2007**, *4*, 4.
(8) (a) De Feyter, S.; De Schryver, F. C. *J. Phys. Chem. B* **2005**, *109*, 4290. (b) Surin, M.; Samori, P. *Small* **2007**, *3*, 190. (c) Yoshimoto, S. *Bull. Chem. Soc. Jpn.* **2006**, *79*, 1167. (d) Tao, F.; Bernasek, S. L. *J. Am. Chem. Soc.* **2005**, *127*, 12750. (e) Nath, K. G.; Ivasenko, O.; MacLeod, J. M.; Miwa, J. A.; Wuest, J. D.; Nanci, A.; Perepichka, D. F.; Rosei, F. *J. Phys. Chem. C* **2007**, *111*, 16996. (f) Zhou, H.; Dang, H.; Yi, J. H.; Nanci, A.; Rochefort, A.; Wuest, J. D. *J. Am. Chem. Soc.* **2007**, *129*, 13774. (g) Bléger, D.; Kreher, D.; Mathevet, F.; Attias, A. J.; Schull, G.; Huard, A.; Douillard, L.; Fiorini-Debuischert, C.; Charra, F. *Angew. Chem., Int. Ed.* **2007**, *46*, 7404. (h) Wei, Y.; Tong, W.; Zimmt, M. B. *J. Am. Chem. Soc.* **2008**, *130*, 3399. (i) Safarowsky, C.; Merz, L.; Rang, A.; Broekmann, P.; Hermann, B. A.; Schalley, C. A. *Angew. Chem., Int. Ed.* **2004**, *43*, 1291. (j) Yoshimoto, S.; Tsutsumi, E.; Honda, Y.; Murata, Y.; Murata, M.; Komatsu, K.; Ito, O.; Itaya, K. *Angew. Chem., Int. Ed.* **2004**, *43*, 3044. (k) Yuan, Q.-H.; Wan, L.-J.; Jude, H.; Stang, P. J. *J. Am. Chem. Soc.* **2005**, *127*, 16279.
(9) (a) Theobald, J. A.; Oxtoby, N. S.; Philips, M. A.; Champness, N. R.; Beton, P. H. *Nature* **2003**, *424*, 1029. (b) Saywell, A.; Magnano, G.; Satterley, C. J.; Perdigão, L. M. A.; Champness, N. R.; Beton, P. H.; O'Shea, J. N. *J. Phys. Chem. C* **2008**, *112*, 7706.
(10) Stepanow, S.; Lin, N.; Vidal, F.; Landa, A.; Ruben, M.; Barth, J. V.; Kern, K. *Nano Lett.* **2005**, *5*, 901.
(11) Langner, A.; Tait, S. L.; Lin, N.; Rajadurai, C.; Ruben, M.; Kern, K. *Proc. Natl. Acad. Sci. U.S.A.* **2007**, *104*, 17927.
(12) Lackinger, M.; Griessl, S.; Markert, T.; Jamitzky, F.; Heckl, W. M. *J. Phys. Chem. B* **2004**, *108*, 13652.
(13) Note that MM simulations indicate that no H-bonds are formed between **ISA** and **COR**; **COR** is stabilized into the **ISA** matrix due to the fact that the geometry of the **ISA** hexagonal network perfectly accommodates one **COR** and the strong interaction of **COR** with graphite.
(14) Blunt, M.; Lin, X.; Gimenez-Lopez, M. D.; Schröder, M.; Champness, N. R.; Beton, P. H. *Chem. Commun.* **2008**, 2304.
(15) Griessl, S. J. H.; Lackinger, M.; Jamitzky, F.; Markert, T.; Hietschold, M.; Heckl, W. M. *Langmuir* **2004**, *20*, 9403.
(16) (a) Barlow, S. M.; Raval, R. *Surf. Sci. Rep.* **2003**, *50*, 201. (b) Ernst, K.-H. *Top. Curr. Chem.* **2006**, *265*, 209. (c) Plass, K. E.; Grzesiak, A. L.; Matzger, A. J. *Acc. Chem. Res.* **2007**, *40*, 287. (d) Katsonis, N.; Lacaze, E.; Feringa, B. L. *J. Mater. Chem.* **2008**, *18*, 2065.
(17) (a) Böhringer, M.; Schneider, W. D.; Berndt, R. *Angew. Chem., Int. Ed* **2000**, *39*, 792. (b) Wei, Y.; Kannappan, K.; Flynn, G. W.; Zimmt, M. B. *J. Am. Chem. Soc.* **2004**, *126*, 5318. (c) Miura, A.; Jonkheijm, P.; De Feyter, S.; Schenning, A. P. H. J.; Meijer, E. W.; De Schryver, F. C. *Small* **2005**, *1*, 131. (d) Zell, P.; Mögele, F.; Ziener, U.; Rieger, B. *Chem.−Eur. J.* **2006**, *12*, 3847. (e) Weigelt, S.; Busse, C.; Petersen, L.; Rauls, E.; Hammer, B.; Gothelf, K. V.; Besenbacher, F.; Linderoth, T. R. *Nat. Mater.* **2006**, *5*, 112.
(18) Tahara, K.; Furukawa, S.; Uji-i, H.; Uchino, T.; Ichikawa, T.; Zhang, J.; Mamdouh, W.; Sonoda, M.; De Schryver, F. C.; De Feyter, S.; Tobe, Y. *J. Am. Chem. Soc.* **2006**, *128*, 16613.
(19) Lei, S.; Tahara, K.; De Schryver, F. C.; Van der Auweraer, M.; Tobe, Y.; De Feyter, S. *Angew. Chem., Int. Ed.* **2008**, *47*, 2964.
(20) Furukawa, S.; Tahara, K.; De Schryver, F. C.; Van der Auweraer, M.; Tobe, Y.; De Feyter, S. *Angew. Chem., Int. Ed.* **2007**, *46*, 2831.
(21) Stöhr, M.; Wahl, M.; Spillmann, H.; Gade, L. H.; Jung, T. A. *Small* **2007**, *3*, 1336.
(22) Schull, G.; Douillard, L.; Fiorini-Debuisschert, C.; Charra, F.; Mathevet, F.; Kreher, D.; Attias, A. J. *Adv. Mater.* **2006**, *18*, 2954.
(23) Dunn, B. M.; Hung, S. H. *Biochim. Biophys. Acta* **2000**, *1477*, 231.
(24) Carloni, P.; Alber, F. *Perspect. Drug Discovery* **1998**, *9−11*, 169.
(25) (a) Self-trapping of **TMA** in its honeycomb networks is observed rarely, both under UHV conditions and at the liquid/solid interface; see: Griessl, S.; Lackinger, M.; Edelwirth, M.; Hietschold, M.; Heckl, W. M. *Single Mol.* **2002**, *3*, 25. (b) Li, M.; Deng, K.; Yang, Y. L.; Zeng, Q. D.; He, M.; Wang, C. *Phys. Rev. B* **2007**, *76*, 155438. In contrast, in the presence of **ISA**, nearly all cavities are occupied (Supporting Information). Therefore, we attribute the molecules trapped inside of the cavities to be **ISA** rather than **TMA**.
(26) Hla, S. W.; Rieder, K. H. *Annu. Rev. Phys. Chem.* **2003**, *54*, 307.
(27) (a) Weigelt, S.; Busse, C.; Bombis, C.; Knudsen, M. M.; Gothelf, K. V.; Strunskus, T.; Wöll, C.; Dahlbom, M.; Hammer, B.; Lægsgaard, E.; Besenbacher, F.; Linderoth, T. R. *Angew. Chem., Int. Ed.* **2008**, *47*, 4406. (b) Grill, L.; Dyer, M.; Lafferentz, L.; Persson, M.; Peters, M. V.; Hecht, S. *Nature Nanotechnol.* **2007**, *2*, 687. (c) Matena, M.; Riehm, T.; Stöhr, M.; Jung, T. A.; Gade, L. H. *Angew. Chem., Int. Ed.* **2008**, *47*, 2414. (d) In't Veld, M.; Iavicoli, P.; Haq, S.; Amabilino, D. B.; Raval, R. *Chem. Commun.* **2008**, 1536.
(28) Koblenz, T. S.; Wassenaar, J.; Reek, J. N. H. *Chem. Soc. Rev.* **2008**, *37*, 247.

NL8016626